



SEISMIC PERFORMANCE OF COLD-FORMED SQUARE-HOLLOW-SECTION STEEL COLUMN TO THROUGH-DIAPHRAGM WELDING CONNECTION USING A 25° NARROW GROOVE

S. Minami⁽¹⁾, K. Hattori⁽²⁾, T. Nakagomi⁽³⁾

⁽¹⁾ Professor, Tokyo Denki University, Japan, minamis@g.dendai.ac.jp

⁽²⁾ Tsukuba Building Test Laboratory of Center for Better Living, Japan, hattori@tblt.org

⁽³⁾ Emeritus Professor, Shinshu University, Japan, nakagom@shinshu-u.ac.jp

Abstract

The welding groove angle and is an important factor that affects the weld quality when welding steel members. Currently, a welding groove angle of 35° is normally used by Japanese fabricators. However, a 25° narrow-groove welding method can improve the production efficiency and reduce the environmental impact. From the previous research results, a welding with a 25° narrow groove is considered to be feasible. However, full-scale tests for this type of groove have not carried out and the performance of a connection welded using a 25° narrow groove has not been evaluated. In this study, we conducted a series of three-point bending tests on a cold-formed square-hollow-structural-section (SHSS) steel column to a through-diaphragm welding connection by using a 25° narrow groove. Subsequently, we investigated the deformation capacity of the welded connection.

The column of the test specimen was a steel rectangular pipe (HSS550x550x32: BCP325) formed by a cold-press forming process. The through-diaphragm of the specimen was made of a steel plate (PL36: SN490C). The length of the support span of the test specimen was 4 m, and the welding groove angle of the test specimen was 25°. A welding robot was used to weld the cold-formed SHSS column and the through-diaphragm. In addition, since the shape of the welded toe has a significant influence on the deformation capacity of the welded connection, the weld toe of one of the specimens was polished using a hand grinder to relieve the stress concentration at the weld toe.

The results obtained in this study are as follows:

- (1) The deformation capacity of a cold-formed SHSS column to a through-diaphragm welding connection by using a 25° narrow groove is comparable to or higher than that obtained in the previous tests conducted using a 35° standard groove.
- (2) In all the test specimens, ductility crack initiation occurred at the weld toe, which did not progress to the heat-affected zone. The crack path was located at the corners of the column. The ductile crack grew, and finally, it induced a brittle fracture in the base material of the column.
- (3) Even when the welding defect existed in the first layer of the column corners, brittle fracture did not occur at the welding defects.
- (4) Relieving the stress concentration at the weld toe with grinder finishing delayed ductile crack initiation, thus improving the deformation capability of the welded connection of the cold-formed SHSS column.

Keywords: cyclic bending loading, cold-formed rectangular steel column, welding robot, plastic deformation capacity



1. Introduction

The root gap and the welding groove angle are important factors that affect the weld quality when welding steel members. Currently, almost all Japanese fabricators follow "the groove standard of full and partial penetration" detailed in the "Japanese Architectural Standard Specification, JASS 6, Steel Work [1]" for the root gap and the welding groove angle. In this standard, a root gap of 7 mm and a groove angle of 35° are adopted as the standard dimensions; hence, these dimensions are normally used by the fabricators.

On the other hand, the 25° narrow-groove welding method [2] improves (a) the production precision by decreasing the welding heat distortion, (b) the environment measures by the reduction of welding materials and the shielding gas (CO₂), and (c) the production efficiency by shortening the arcing time. Currently, the main application of a welding robot involves girth welding of column members in steel building structures.

Recently, the structural system using cold-formed square-hollow-structural-section (SHSS) steel as column members and using H-shaped steel as beam members is adapted to a large number of medium- to high-rise steel buildings. Since the diffusion of welding robots is very high for a cold-formed steel SHSS column to a through-diaphragm welding connection, we focused the investigation of the study on this type of welding connection.

From the previous research results [3–5], welding with a 25° narrow groove is considered feasible. However, a full-scale test has not been carried out, and the performance of a column to a through-diaphragm connection welded using a 25° narrow groove has not been studied. In this study, the authors carried out a series of three-point bending tests on a cold-formed SHSS steel column to a through-diaphragm welding connection by using a 25° narrow groove and clarified the deformation capacity and the fracture condition of the welded connection.

2. Experimental outline

2.1 Test specimen

Fig. 1 illustrates the shape of the test specimen and the details of the connection. The specifications of the test specimens are listed in Table 1. The cold-formed SHSS column of the specimen was a rectangular steel pipe (HSS550x550x32; BCP325) formed by a cold-press forming process. The through-diaphragm of the specimen was made of a steel plate (PL36; SN490C). The floor height of the building is assumed to be 4 m, and so the length of the support span of the test specimen was set to 4 m. The groove angle of the welding connection between the column and through diaphragm of the test specimen was 25°. A welding robot was used for the welding process.

Table 1 – Specifications of test specimens

No.	Size B x t	Steel material	G.A.	R.G. (mm)	Test temperature	cM_p (kN·m)	cP_p (kN)	$c\delta_p$ (mm)	Artificial defect depth/length	Weld toe finish
CP-1	550x32	BCP325	25°	4	0°C	4404	4404	11.1	–	as welded
CP-2				8					6 mm/48 mm	polished
CP-3				8					6 mm/48 mm	as welded

B: Side dimensions (mm), **t:** Nominal wall thickness (mm), **G.A.:** Groove angle, **R.G.:** Gap at the root opening,

cM_p : Full plastic moment (computed value), cP_p : Load at full plastic moment (computed value),

$c\delta_p$: Elastic component of displacement at full plastic moment (computed value),

All the values are computed using the test results on the yield point of the materials at 0 °C.

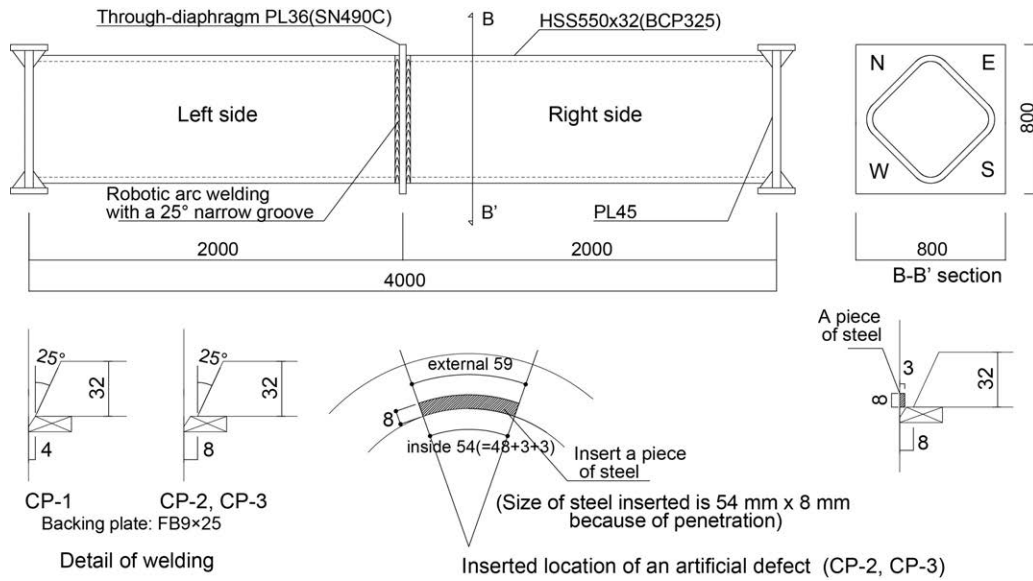


Fig. 1 – Test specimens (dimensions are in mm)

Because the 25° narrow groove had a smaller cross section than the 35° standard groove, it was expected to induce large welding defects in the first layer on the diaphragm side. To examine the effects of welding defects in the first layer on the deformation capacity of the welded connection, in CP-2 and CP-3 test specimens, welding defects were artificially induced in the first layer on the diaphragm side (target dimensions: defect depth = 6 mm, defect length = 48 mm, the details are shown in Fig. 1).

In addition, the shape of the welded toe has a significant influence on the deformation capacity of the welded connection. The weld toe of one of the specimens was polished using a hand grinder to relieve the stress concentration at the weld toe.

2.2 Mechanical properties of material used

The tensile and Charpy impact tests were carried out to obtain the mechanical properties of the material used. The tensile test was conducted in accordance with JIS Z 2241:2001 (Metallic materials-Tensile testing method of test at room temperature). The test temperature was set at 0°C, the same as that used in the full-scale bending test. The test piece for the side wall of the column was No.1A-type and that for the corner part was No.14B-type. For the weld deposited metal, the test piece was No.A2-type of JIS Z 3111:2005 (Methods of tension and impact tests for deposited metal). The test results are presented in Table 2. The chemical components in Table 2 were obtained from the Mill sheets.

Table 2 – Mechanical properties and chemical components

Steel material	Part	σ_{y1} N/mm ²	σ_{y0} N/mm ²	σ_u N/mm ²	Y.R. %	EL. %	T °C	$\sqrt{E_0}$ J	C	Si	Mn	P	S	Ni	Cr	Mo	V	N	Ceq
									x100	x1000	x100			x10000	x100				
BCP325	Side	364	-	528	69	-	0	287	15	22	146	9	2	2	2	0	6	52	41
	Corner	-	475	558	85	-	0	224	-	-	-	-	-	-	-	-	-	-	-
Weld metal		561	-	568	85	34	0	47	-	-	-	-	-	-	-	-	-	-	-
SN490C	DF	385	-	577	69	43	0	290	17	38	131	14	4	2	2	1	0	-	41

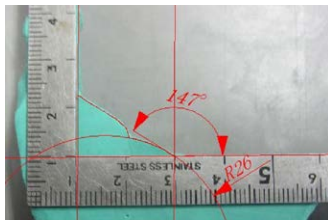
DF: Diaphragm, σ_{y1} : Lower yield strength, σ_{y0} : Proof strength, σ_u : Tensile strength, Y.R.: Yield ratio, EL.: Elongation, T: Test temperature, $\sqrt{E_0}$: Charpy absorption energy at 0 °C, Ceq = C+Mn/6+Si/24+Ni/40+Cr/5+Mo/4+V/14

2.3 Artificial weld defect

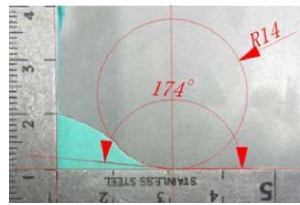
The welding defects were made artificially in CP-2 and CP-3 test specimens. The dimensions of the artificial weld defect were set to the maximum allowable size limit in "AIJ: Standard for the Ultrasonic Inspection of Weld Defects in Steel Structures [6]" (often referred to as the "AIJ UT Standard"). The defects were 6 mm deep and 48 mm long. As shown in Fig. 1, a steel plate of thickness 3 mm was inserted in each corner part of the column before welding, so that incomplete penetration occurs on the faces where the metal touches.

2.4 Shaping of the weld toe

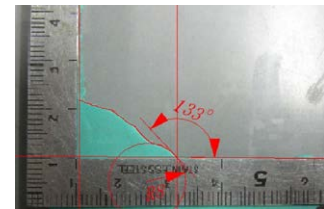
The shapes of the weld toe at each corner of the column were obtained by using a dental impression material before the loading test. The sectional shapes are shown in Fig. 2. The specimen CP-2 was polished using a hand grinder, and the specimens CP-1 and CP-3 were not finished and were in the as-welded condition. The flank angle of CP-1 was 147° and that of CP-3 was 133° . The flank angle of CP-2 was 174° larger than that of the other specimens.



CP-1 (as welded)



CP-2 (polished)



CP-3 (as welded)

Fig. 2 – Shape of weld toe

3. Experimental method

The loading direction of the square section of the column was at 45° to the extreme conditions for the column. Fig. 3 shows the experimental setup. Using a hydraulic-type testing machine with a 10 MN capacity, the specimen was subjected to static bending loading using displacement control. The loading program is shown in Fig. 4. The loading was applied following the incremental amplitude procedures. The displacement amplitudes for control were $\pm 0.5\delta_p$, $\pm 2\delta_p$, $\pm 4\delta_p$, $\pm 6\delta_p$, and $\pm 8\delta_p$, as computed using Eqs. (1)–(5), respectively, in Fig. 3.

The test temperature in this experiment was set at 0°C . As shown in Fig. 3, a refrigerant consisting of ethanol cooled by dry ice particles was supplied into the column to cool the specimen during the test. An insulation material was wrapped around the specimen to prevent heat discharge radiation from the specimen. The temperature of the specimen was controlled by a thermocouple at $0 \pm 5^\circ\text{C}$.

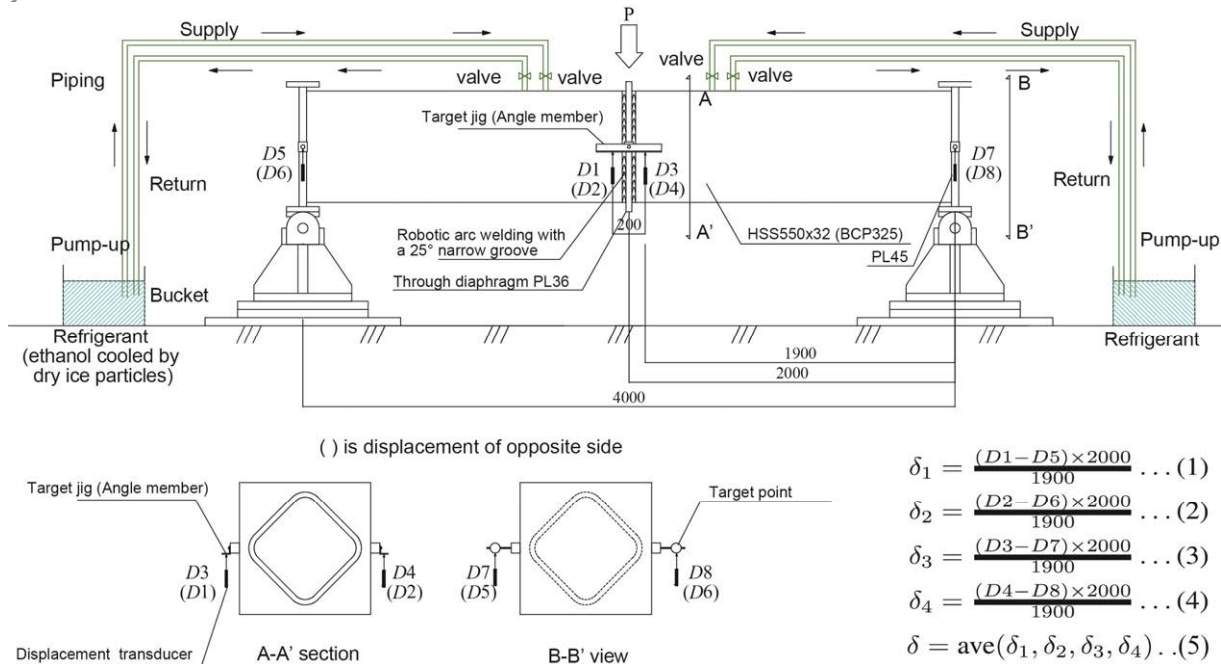


Fig. 3 – Experimental setup

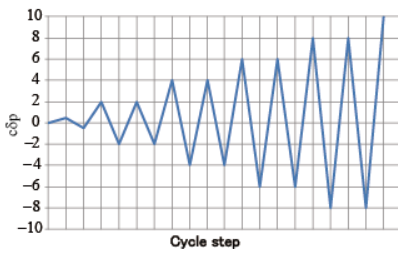


Fig. 4 – Loading program



Fig. 5 – Loading test condition

4. Experimental results

4.1 Load–displacement relationship

The test results are presented in Table 3. Fig. 6 shows the relationship between load and displacement. The red line indicates the skeleton curve. The specimen CP-2 did not fracture at $8_c\delta_p$ but fractured subsequently. CP-1 and CP-3 exhibited a brittle fracture at $8_c\delta_p$ and $6_c\delta_p$, respectively.

Table 3 – Test results

No.	Fracture cycle	eP_p (kN)		eP_{max} (kN)		$c\delta_p$ (mm)		α		$e\eta_s$		$e\eta_A$		Fracture condition	Note
		+	-	+	-	+	-	+	-	+	-	+	-		
CP-1	-8 (1st)	4143	-3815	5661	-5494	80.1	-65.5	1.29	1.25	10.0	8.0	38.7	40.8	DB	
CP-2	Push-over	4435	-4087	6356	-6148	191.1	-87.7	1.44	1.40	24.9	15.0	83.8	63.4	DB	Local buckling
CP-3	-6 (2nd)	4156	-3826	5620	-5563	67.7	-65.7	1.28	1.26	8.6	8.2	27.4	28.3	DB	

Note: eP_p : Load at full plastic moment (experimental result by the general yield method), eP_{max} : Maximum load (experimental result), $e\delta_{max}$: Maximum displacement (experimental value), α : Maximum strength ratio ($=eP_{max} / eP_p$), $e\eta_s$: Cumulative plastic deformation based on the skeleton curve, $e\eta_A$: Total cumulative plastic deformation, "DB": Brittle fracture in the base material of column corner after the growth of the ductile crack.

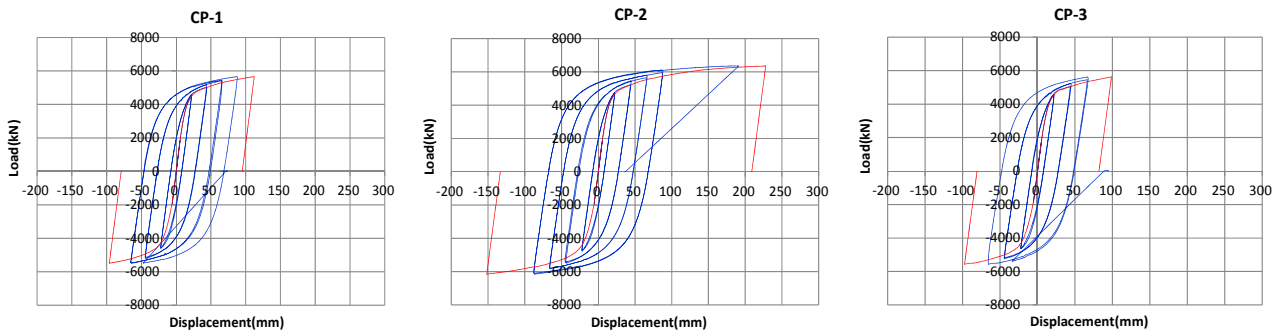


Fig. 6 – Load–displacement relationship

4.2 Fracture behavior

Photos of the fractured specimen are shown in Fig. 7. In all the specimens, ductility crack initiation occurred at the weld toe during cyclic loading. Next, the ductile crack grew into the corners of the column, and finally, the ductile crack induced brittle fracture of the base material of the column. The ductility crack did not propagate to the heat-affected zone, but the crack path was located in the base material of the column.



Fig. 7 – Photos of the fractured specimen

5. Discussions

5.1 Cumulative plastic deformation

The cumulative plastic deformation $\epsilon_{\eta A}$ can be determined by the sum of all hysteresis load–displacement relation curve obtained from the experimental result. In addition, $\epsilon_{\eta S}$ was determined by the skeleton curve. These values are shown in Table 3.

Table 4 shows the requirement value of the plastic deformation capacity for the column member as per Ref.[7]. R_{η} is the demand cumulative plastic deformation capacity of a story for the moment frame. Because the width-thickness ratio B/t is 17 in this specimen, the requirement value of cumulative plastic deformation capacity for the column, $\epsilon_{\eta S}$, is 8.4 for the skeleton and 14 for the total energy of one side.

Figs. 8 and 9 show the comparisons of the test results. The value in the fractured side was adopted for $\epsilon_{\eta S}$. $\epsilon_{\eta A}$ is the sum of the positive and negative values. $\epsilon_{\eta A}$ satisfied the requirement value for the column member, as shown in Table 4; however, $\epsilon_{\eta S}$ does not satisfy the requirement adequately, albeit slightly.

Table 4 – Requirement of plastic deformation capacity for a column

Structural Rank	for Frame	for Column				for References	
	Demand	Brittle fracture		Local buckling, others		Ds (Column collapse type)	Limit of B/t
	$\epsilon\eta$	$\epsilon\eta_s$	$\epsilon\eta_A$	$\epsilon\eta_s$	$\epsilon\eta_A$		
I	7.00	8.4	14	6	10	0.3	23
II	3.25	3.9	6.5	1.5	2.5	0.4	28
III	2.00	2.4	4	0	0	0.5	41
IV	1.00	1.2	2	0	0	0.6	–

$\epsilon\eta$: Cumulative plastic deformation capacity for the moment frame,
 $\epsilon\eta_s$: Requirement of plastic deformation capacity for the skeleton curve of the column,
 $\epsilon\eta_A$: Requirement of plastic deformation capacity for the total hysteresis curve of the column,
B/t: Width-thickness ratio of the column.

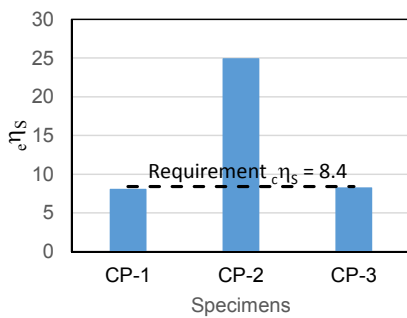


Fig. 8 – Estimation of test results ($\epsilon\eta_s$)

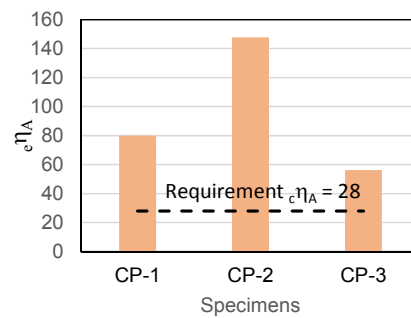


Fig. 9 – Estimation of test results ($\epsilon\eta_A$)

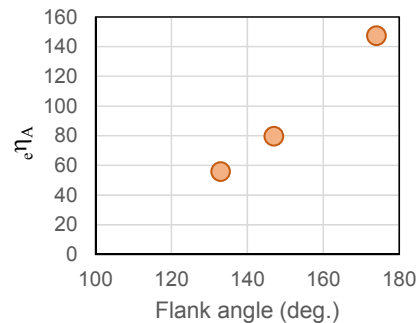
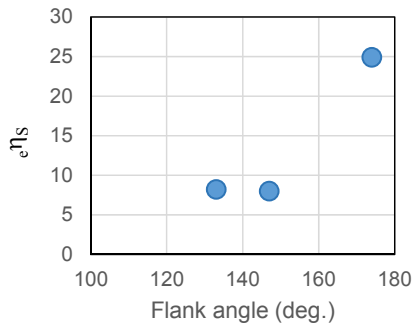


Fig. 10 – Relation between plastic deformation and flank angle

The relationship between cumulative plastic deformation and the flank angle is shown in Fig. 10. Clearly, the larger the flank angle, the higher the performance of the plastic deformation.

Even when the existing weld defect size in the first layer of the column corner was acceptable, according to the maximum limit indicated in the AIJ UT Standard, brittle fracture did not occur from the weld defect. The reason is that the stress and strain inside the column corner are smaller than those at the outside. The critical point of fracture was the corner outside, and not the side of the first layer, as previously reported Ref. [8].

5.2 Comparison with performance of weld method by using a 35° conventional groove

Fig. 11 compares the performance of several weld methods by using a 35° conventional groove [9, 10] with that of the proposed method. The line in the figure indicates the required performance when the yield strength is 325 N/mm², which is the specified value of the BCP325 steel material. In the figure, the circular marks indicate our test results with a 25° narrow groove, while the diamonds marks denote past test results at a 35° conventional groove. In all test results, the loading direction was 45°. The tests at 35° groove were carried out at room

temperature. The specimen CP-2 seems to have exhibited high performance. The two other specimens exhibited almost the same performance as the past test results.

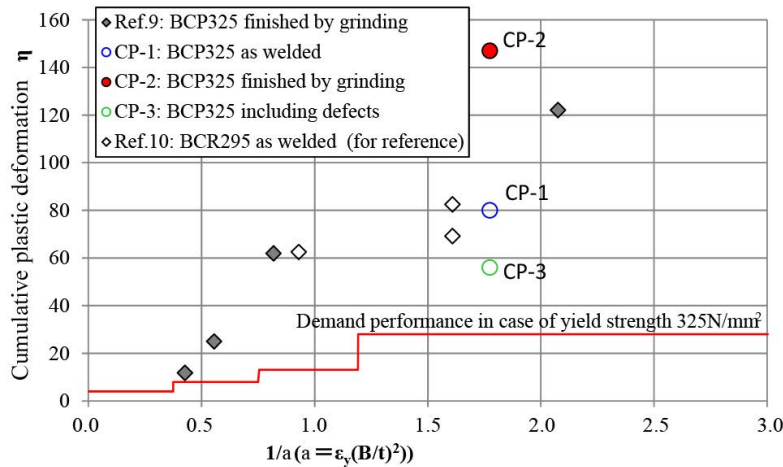


Fig. 11 – Comparison with test results from past studies

6. Conclusions

The results obtained in this study are as follows:

- (1) The deformation capacity of a cold-formed SHSS column to a through-diaphragm welding connection using a 25° narrow groove is comparable to or higher than that obtained in previous tests using a 35° standard groove.
- (2) In all the test specimens, ductility crack initiation occurred at the weld toe. The ductility crack did not propagate to the heat-affected zone. The crack path was located in the corners of the column. The ductility crack grew, and finally, it induced a brittle fracture in the base material of the column.
- (3) Even when a welding defect existed in the first layer of the column corners, brittle fracture did not occur from the welding defect.
- (4) Relieving the stress concentration at the weld toe through grinder finishing delayed ductile crack initiation, thus improving the deformation capability of the welded connection of the cold-formed SHSS column.

7. Acknowledgements

This study was conducted in cooperation with the Japanese Society of Steel Construction, Japan Steel Fabricators Association, and Japan Iron and Steel Federation as part of the “Technical development of automatic arc welding for advancing structural safety of steel buildings” (Chairman; Dr. Kohji Morita, Emeritus Professor, Chiba University) using subsidy granted by the Ministry of Land, Infrastructure, Transport and Tourism. The authors would also like to thank students of the Shinshu University, the Tokyo Metropolitan University, and the Chiba Institute of Technology for their support in this experiment.

8. References

- [1] Architectural Institute of Japan (2007): *Japanese Architectural Standard Specification*, JASS 6, Steel Work.
- [2] Japan Steel Fabricators Association (2006): *The 25° Single Bevel Narrow Groove Welding Method Manual*.



- [3] Hiroshi Matsumura, Tadao Nakagomi, Shigeto Takada (2010): A study on the welding procedure of the first layer of the narrow groove welding for steel frames of buildings by welding robots, *Journal of the Japan Welding Society*, Japan Welding Society, **28** (1), 39-47.
- [4] Hiroshi Matsumura, Tadao Nakagomi (2011): A Study on the Welding Procedures of Narrow Groove Welding for Square Steel Tube Columns by Welding Robots, *Journal of Structural and Construction Engineering (Transaction of AIJ)*, Architectural Institute of Japan, **76** (664), 1059-1067.
- [5] Tatsuya Nakano, Hiroshi Matsumura, Kazuo Watanabe, Ichiro Chishiro, Koji Morita (2013): Range of Conditions on Built-up Welding and First Layer Welding in Narrow gap with 25 Degree Single Bevel Groove - Technical development of automatic arc welding in narrow gap with single bevel groove for cold formed SHS column to through-diaphragm connection Part 1, *Journal of Structural and Construction Engineering (Transaction of AIJ)*, Architectural Institute of Japan, **78** (686), 647-656.
- [6] Architectural Institute of Japan (2008): *Standard for the Ultrasonic Inspection of Weld Defects in Steel Structures*.
- [7] Building Research Institute and Kozai Club (1993): Research Report of Column Design Committee ~ Evaluation of cold-formed steel column from the point of view of requirement and capacity as column member in steel frame building structures.
- [8] Shunichi Takagi, Tatsuya Nakano, Haruhito Okamoto, Tomoya Kato (2011): FEM analysis on stress and strain behavior of robotic arc welding connection using 25 degree acute bevel angle (Part 1 - Part 2), Summaries of Technical Papers of Annual Meeting, Architectural Institute of Japan, A-1, 1065-1068.
- [9] Shinya Inaoka, Haruhito Okamoto, Fumihiko Imai, Shun Sasajima, Ryoji Endo (1998): An Experimental Study on New Cold-Formed Box-Section Columns (Part 1 - Part 2), Summaries of Technical Papers of Annual Meeting, Architectural Institute of Japan, C-1, 687-690.
- [10] Toru Motoda, Masao Sonoda (1999): Experimental Study on Bending Behavior of Cold-Formed Rectangular Hollow Section Appropriate for Building Structure (Part 3), Summaries of Technical Papers of Annual Meeting, Architectural Institute of Japan, C-1, 365-366.